AGU PUBLICATIONS

Geophysical Research Letters

RESEARCH LETTER
10.1002/2015GL063433

Key Points:
- Jupiter mesoscale waves propagate 90 m/s eastward relative to cloud level winds
- Wave velocities, wavelength, and latitude extent are consistent with Kelvin waves
- Wave lifetimes may exceed 2 h in Voyager and New Horizons images

Supporting Information:
- Table S1 and Figure S1

Correspondence to:
A. A. Simon,
amy.simon@nasa.gov

Citation:
Simon, A. A., L. Li, and D. C. Reuter (2015), Small-scale waves on Jupiter: A reanalysis of New Horizons, Voyager, and Galileo data, *Geophys. Res. Lett.*, *42*, doi:10.1002/2015GL063433.

Received 9 FEB 2015
Accepted 26 MAR 2015
Accepted article online 28 MAR 2015

Small-scale waves on Jupiter: A reanalysis of New Horizons, Voyager, and Galileo data

A. A. Simon[1], L. Li[2], and D. C. Reuter[1]

[1]NASA Goddard Space Flight Center, Greenbelt, Maryland, USA, [2]Physics Department, University of Houston, Houston, Texas, USA

Abstract Jupiter's equator-encircling mesoscale waves were a distinguishing feature observed during the New Horizons Jupiter flyby. Measured velocities indicated eastward propagation, inconsistent with standing wave models developed after the Voyager encounters. We present revised New Horizons mesoscale wave velocities of 164 to 176 m/s, approximately 90 m/s higher than the tropospheric zonal winds on that date, while Voyager and Galileo mesoscale waves do not show any apparent motion. This is consistent with an eastward propagating inertia-gravity or Kelvin wave, or a wave propagating with the wind at certain altitudes, given proper vertical wind shears. New Horizons high solar phase angle methane band observations show wave crest shadows or aerosol clearing, implying altitudes above the cloud deck for the observed features. New Horizons and Voyager data also indicate that wave trains have lifetimes exceeding two Jovian rotations.

1. Introduction

Mesoscale waves were first seen in Jupiter's atmosphere in Voyager images [*Flasar and Gierasch*, 1986]. Packets were seen at many latitudes, but most were near the equator, with wavelengths ranging from 166 to 422 km and an average of about 300 km. In some cases packets were seen in the same area in more than one frame, but it was not possible to confirm if it was the same wave train or to constrain wave velocities, due to the lack of distinguishable features within the wave trains. Modeling these features as standing waves in the cloud deck fit the observations; however, the wave lifetime, altitude, and phase velocity were not well constrained by the Voyager data [*Flasar and Gierasch*, 1986; *Bosak and Ingersoll*, 2002] and other data sets were needed.

Similar waves were apparently rare during the Galileo spacecraft epoch (1995–2003); for example, despite dedicated high-resolution imaging sequences, *Arregi et al.* [2009] reported only three wave packets within 3° of the equator visible in 1999 and 2001, with few seen anywhere else during the mission (image release PIA00490 shows another such packet from 1996). No mesoscale waves were observed in Cassini flyby data from late 2000.

However, in 2007, large wave trains were seen in New Horizons Ralph/Multicolor Visible Imaging Camera (MVIC) image frames, spanning nearly the entire longitude range of the equatorial region [*Reuter et al.*, 2007]. Compared to Voyager measurements, the New Horizons waves had a much more consistent wavelength of ~305 km and much larger packet sizes, but they were more constrained in latitude to within a few degrees of the equator. The New Horizons data included short time separation views over a long span of longitude, which allowed a few unique wave crests to be identified and permitted velocity measurements. These images were reported to have been taken at UTs of 06:00, 06:26, and 06:41 and yielded a wave velocity of 220 to 250 m/s, 120+ m/s higher than the background clouds [*Reuter et al.*, 2007]. The waves were visible in all the New Horizons Ralph/MVIC filters [*Reuter et al.*, 2008] but were most apparent in the narrow methane absorption (889 nm) band, in part because that was the only filter not saturated away from the terminator. The waves were also visible in the high-spatial resolution LORRI panchromatic channel [*Reuter et al.*, 2007; *Cheng et al.*, 2008]. Table 1 shows a summary of observed wave properties from each of these missions.

In this paper, we present a reanalysis of the spacecraft data described above. First, we use the updated times of the New Horizons MVIC frames, to determine the wave velocity for comparison to other data sets, including Galileo images. Second, we attempt to constrain the altitude of the waves via the thermal wind equation, the optical passbands of the various filters in which they were observed, and shadow observations. These values are then compared with a reanalysis of Voyager 2 images. Finally, we attempt to reconcile the observed data with analytic models.

Table 1. Observed Mesoscale Waves

Spacecraft	Wave Graphic Latitude	Wavelength (km)	Phase Velocity[a] (m/s)	Source
Voyager 1979	$< \pm 30°$	300 ± 130	Unknown	*Flasar and Gierasch* [1986]
Galileo 1996	$-15°$	300	Unknown	*Bosak and Ingersoll* [2002]
Galileo 1999	3.2°	180 ± 25	35 ± 8	*Arregi et al.* [2009]
Galileo 1999	0.2°	205 ± 10	8 ± 8	*Arregi et al.* [2009] and this work
Galileo 2001	$-2.1°$	110 ± 20	0 ± 8	*Arregi et al.* [2009]
New Horizons 2007	0°	305 ± 25	80 ± 5	*Reuter et al.* [2007] and this paper

[a]Relative to the background zonal wind flow, positive indicates eastward.

2. Wave Velocity

In *Reuter et al.* [2007], the New Horizons Ralph/MVIC frames were reported to have been taken at UTs of 06:00, 06:26, and 06:41, which, when compared with the distances identifiable features had moved during that time, yielded a wave velocity of 220–250 m/s [*Reuter et al.*, 2007]. However, the frame times were later determined to be 06:00, 06:41, and 06:55. With this new timing, the velocity is found to be 164 to 176 m/s, see Figure 1. Though there are relatively few equatorial clouds from which to measure the background zonal winds in the New Horizons data, they have velocities ~65–95 m/s, confirmed by measurements on near-simultaneous Hubble data from February to March 2007.

The MVIC frames show the wave trains over extensive longitudes acquired during scans with ~46 km/pixel spatial resolution. Although not acquired concurrently, New Horizons LORRI frames also imaged Jupiter throughout the flyby, see supporting information Table S1. With exquisite spatial resolutions of 11–12 km/pixel, the wavelength was found to be 305 ± 25 km [*Reuter et al.*, 2007]. Waves are seen in all LORRI images of the equator within half a day of closest approach, but the same longitudes were imaged neither by LORRI in each sequence nor by both MVIC and LORRI, preventing velocity measurements. The wave packets in the LORRI frames have a peak to trough contrast of ~3–7%, similar to that seen in the MVIC data [*Reuter et al.*, 2007].

The New Horizons measured velocity is still somewhat higher than the velocities reported by *Arregi et al.* [2009] who found the Galileo wave packet closest to the equator to have nearly zero phase velocity, and a wave near 3°S to have a phase velocity of $\sim 35 \pm 8$ m/s. We analyzed the Galileo C20 wave feature track sequence images that had a spatial resolution of ~21 km/pixel using the same methods used to analyze the New Horizons images. Navigated maps were high-pass filtered to remove background clouds and to enhance the wave crests, Table S1. Each mapped frame was used for short (15 min) and long (30 min) separation correlations. In agreement with *Arregi et al.* [2009], no high-velocity motions are detected. Wave crest separations were also measured, yielding an average wavelength of 209.5 km, again in agreement with *Arregi et al.* [2009].

3. Wave Altitude

It is unclear if the waves exist within the tropospheric cloud deck, above it, or below it. Proper radiative transfer retrievals to determine feature altitudes require simultaneous emission angle and filter coverage (methane gas absorption and continuum bands) that is not available in these data sets. The waves are clearly visible in New Horizons MVIC methane filter images, which could indicate higher altitudes than the base cloud deck, although deeper features are often visible at these wavelengths. Velocities found from these images imply a wave velocity higher than the observed cloud deck zonal winds, or eastward propagation, while standing waves would have the same velocity as the wind field at some altitude. This statement may not be contradictory, if the waves exist at an altitude with higher zonal wind velocity than the tropospheric cloud deck velocities. This type of vertical wind shear is possible because of a vertical oscillation in temperature near the equator, Jupiter's QuasiQuadrennial Oscillation (QQO) [*Leovy et al.*, 1991; *Orton et al.*, 1991; *Simon-Miller et al.*, 2006].

The QQO has a period of ~4 to 5 Earth years, averaging 4.5 years, as measured from Voyager, Cassini, and ground-based temperature oscillations in Jupiter's stratosphere [*Simon-Miller et al.*, 2006]. Using the

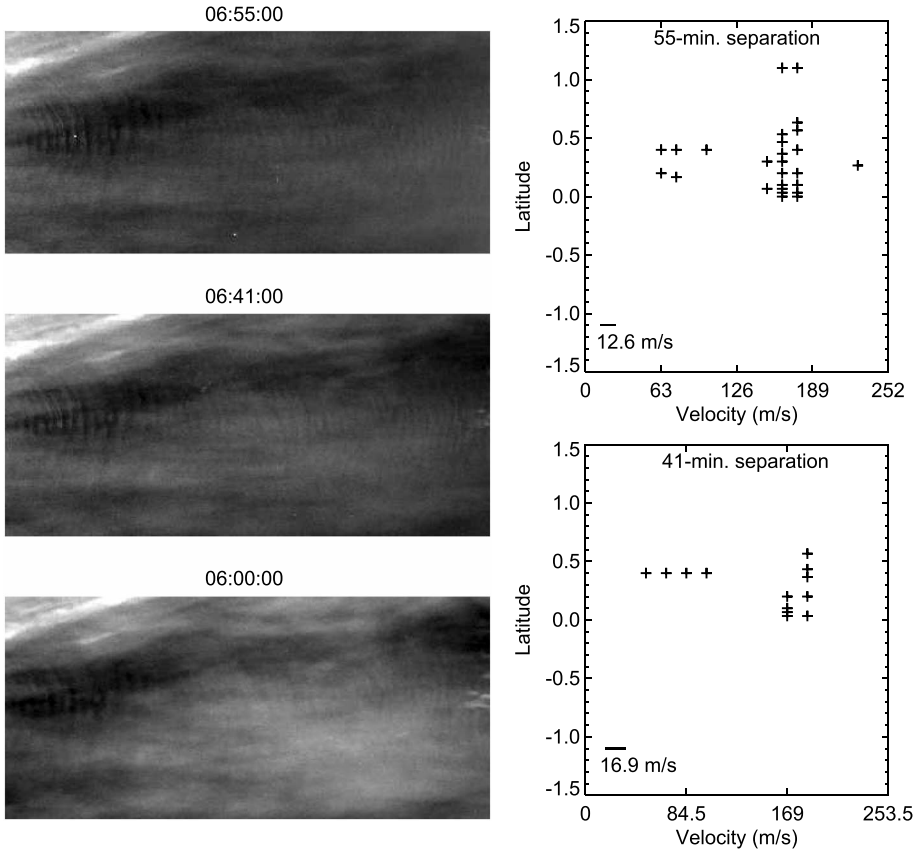

Figure 1. Correlation plots for New Horizons MVIC methane band images with 41 and 55 min separations. Small background cloud features (left set of crosses) have velocities of 65–95 m/s, while the velocities of the wave trains (right set of crosses) are near 170 m/s.

retrieved temperature profiles, the thermal (gradient) wind equation can be used to calculate vertical wind shear. Typically, this equation is given in the standard form based on geostrophic balance, which fails near the equator as the Coriolis parameter approaches zero [e.g., *Salby*, 1996]. However, a more generalized form that integrates along a cylindrical path, rather than radially, can be used to retrieve wind shears closer to the equator near the base wind field, with interpolation to the equator at higher altitudes [*Li et al.*, 2013, Supplementary Material].

The QQO phase at the time of the Cassini flyby (late 2000) was such that the horizontal velocities at cloud deck near 500 mbar were at a maximum, with a minimum velocity near 30 mbar, Figure 2b. Assuming a 4.5 year period, the phase of the QQO would be ~280° offset during the Voyager flybys (early to mid 1979) compared with Cassini, such that the temperature and wind oscillations are not as strong and the minimum near 30 mbar is not as pronounced. The QQO period is variable, and nearly any phase could have been present, but a phase offset is confirmed by retrieved Voyager InfraRed Interferometer Spectrometer (IRIS) temperatures [*Simon-Miller et al.*, 2006] and their corresponding thermal winds, Figure 2a.

Given the relatively short time (6.25 years) between Cassini and New Horizons, the 4 to 5 year oscillation period range means the New Horizons flyby occurred at ~144° to 202° phase offset relative to Cassini. This would mean that the temperature profile is approximately the opposite phase of the QQO, giving a nearly inverted vertical shear profile from Cassini; an increase in zonal wind speed with altitude is expected. Using the Cassini profile as a proxy, the wind shear with altitude is such that a 90 m/s change in velocity relative to the 500 mbar cloud deck occurs at a pressure between 112 and 141 mbar (1.3 to 1.5 scale heights above the cloud deck). The exact altitude may vary slightly from this range given that the QQO phase offset may not be exactly 180°. Thus, the wave altitude could be in the upper troposphere, well above the top of the ammonia cloud deck, although it is unlikely we would observe cloud features this

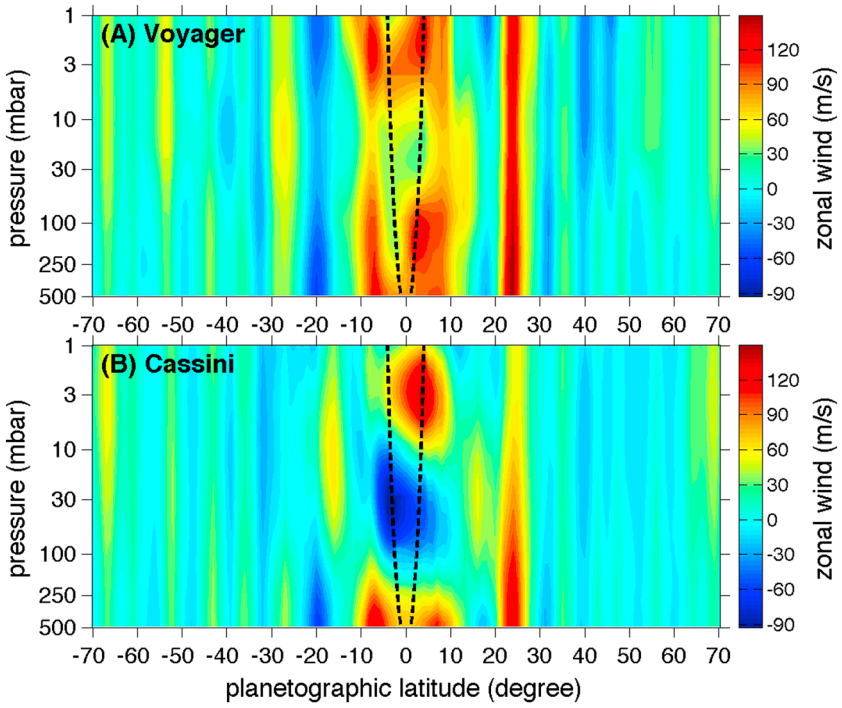

Figure 2. Jupiter's zonal winds calculated from the thermal wind equation as a function of altitude during (a) Voyager and (b) Cassini eras. Equatorial areas are interpolated between the dotted lines and have uncertainties on the order of ~20 m/s. These retrievals show the presence of the equatorial wind oscillation from the QQO.

high above the cloud deck. The other possibility is that the waves come from relatively deep layers (i.e., ammonium hydrosulfide and water clouds), in which the zonal winds are probably stronger than the winds at the ammonia cloud deck [*Atkinson et al.*, 1997, 1998; *Li et al.*, 2006] and close to the observed wave velocities (164–176 m/s).

Although the absolute altitude is difficult to determine from wind shear, some of the waves in the LORRI frames very close to the terminator appear to have shadows (see Figure 3b). These span ~4 pixels, or ~44.7 km, and so are too small to be resolved in the Voyager or MVIC data, and only appear at the highest phase angles, and thus are not observed in the Galileo data. Translating shadow height to wave crest amplitude is not straightforward as it is highly dependent on the exact solar zenith angle for these oblique views; the images are near the terminator and the subsolar latitude was ~2.9°S. Given the pointing uncertainties and lack of limb for navigation, the exact angle is between ~88.7° and 89°, corresponding to heights of .78 to 1.0 km. The actual height also depends on the projection range to the background clouds, which is unknown. Finally, the feature may not even be a shadow, but an aerosol clearing as atmosphere parcels rise and ices condense out to make the wave crests. In either case the fact that such structures are visible may favor that the waves are above the local main cloud deck. No known cloud deck feature casts such a clear shadow. The most similar feature would be the Saturn polar vortex eye wall, observed by Cassini at high solar angles [*Dyudina et al.*, 2009].

4. Reanalysis of Voyager Data

Flasar and Gierasch [1986] identified a large number of Voyager 1 and 2 frames with wave packets, with waves observed more often in the orange channel than in the violet. Independently searching through the Planetary Data System, we identified Voyager 2 Imaging Science Subsystem (ISS) orange frames of the same approximate latitude and longitude regions. While some wave trains may extend over a substantial longitude range, contrast was insufficient in most frames to determine if they were as extensive as in New Horizons (Figures 3a and 3b). From the full Voyager set, we found four frames with time separations of 30 min to 10 h (see Table S1).

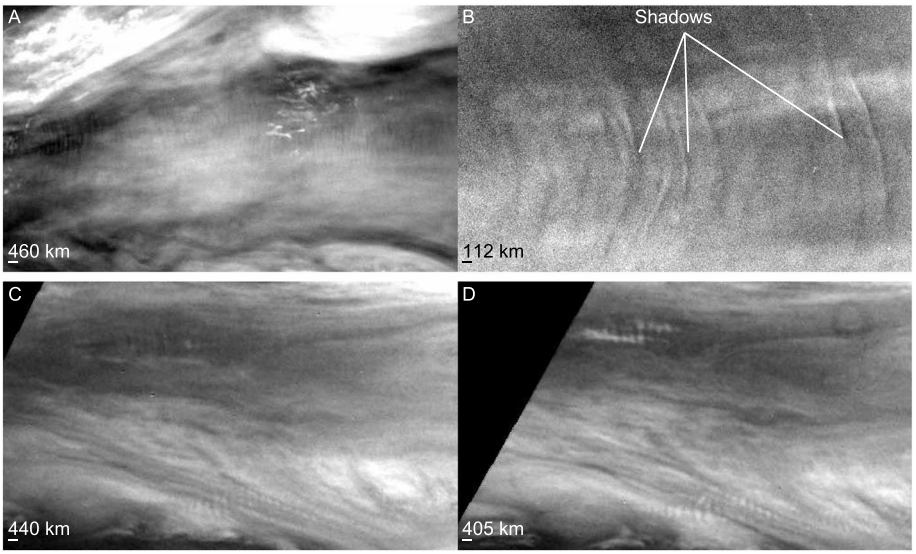

Figure 3. Comparison of New Horizons MVIC and LORRI and Voyager 2 ISS wave packets in unmapped images. (a) An MVIC methane band image showing extensive wave trains centered at the equator at roughly 46 km/pixel resolution. (b) A LORRI panchromatic image showing wave trains near the terminator, with possible shadow features, at roughly 11.2 km/pixel resolution. (c) An ISS orange channel image centered near 2.5°S at ~44 km/pixel resolution shows wave packets near the equator and 5°S latitude. (d) Same region as Figure 3c but ~10 h later and at 40.5 km/pixel resolution.

These frames had waves visible at the equator, with another train apparent near ~5°S planetographic latitude, see Figures 3c and 3d. Images were approximately navigated and were then used to predict wave crest locations using the wave velocities determined from the New Horizons data. If the equatorial wave packet is propagating eastward at ~165 m/s, a crest will have moved 287 km (0.23° of longitude or ~14 pixels in our mapped data) in 29 min and 6108 km (4.9° or 294 pixels) in 10 h 17 min. Even without absolute navigation, the motion against the background clouds would be substantial over 10 h (~143 pixels).

No obvious motion is detectable in the short time separation image pairs, and although a few cloud features can be vaguely matched in the 10 h time separation, there is not enough contrast in the equatorial features to make a positive identification of wave crests. The wave packet at 5°S may show slight evidence of motion, but the background wind velocities are also higher, and they are thus inconclusive in studying the motion of the equatorial waves.

However, the fact that wave packets are seen near the same latitude and longitude regions in each of the Voyager images gives some evidence that the wave packet lifetime can be at least two Jovian days and possibly longer. The Galileo wave feature track only covers about 2 h, as well, with only slight evidence of waves in other images 10 h apart [*Arregi et al.*, 2009]. Due to the rapid flyby of New Horizons, there are limited data with sufficient spatial resolution repeated over the same longitudes and over multiple Jovian rotations, but the waves observed in LORRI at different longitudes span 20 h of observation.

5. Comparison to Wave Models

Flasar and Gierasch [1986] proposed a ducted gravity wave model, in which the waves propagate in a stable layer extending 20–26 km downward from the base of the ammonia cloud. The ammonia clouds above and the convective interior below act as wave trapping regions because of their low static stability and the evanescent behavior of waves in these regions. Since the waves propagate horizontally, their phase speed does not have to match the local wind speed. The theory predicts a discrete set of phase speeds corresponding to the different vertical modes of the duct. Forcing in a narrow frequency range is needed to explain the preferred horizontal wavelength, and they propose that the waves are externally forced at the diurnal frequency.

Bosak and Ingersoll [2002] proposed a shear instability model, in which the waves arise spontaneously in a layer of relatively high shear and low static stability (i.e., Richardson number $< 1/4$). There is no external

forcing. The preferred horizontal wavelength is related to the thickness of the shear layer, which is obtained from the wind measurements obtained with the Galileo probe [*Atkinson et al*., 1998]. The fastest growing waves grow exponentially within an hour, and for a shear layer 46 km thick from 3 to 10 bars they have wavelengths of 240–290 km, which matches the observed wavelengths. The phase speeds of the fastest growing waves are intermediate between the wind speeds at the top and bottom of the shear layer, which at the Galileo probe site were 70 and 180 m s^{-1}, respectively.

The models describe two fundamentally different mechanisms, and they have different observational consequences. First, ducted gravity waves (DGWs) can propagate faster or slower than the wind, whereas shear instability waves (SIWs) do not propagate but are stationary with the wind at some altitude within the shear layer. Second, DGWs that are diurnally forced should have coherent crests and troughs at least for one Jovian day and probably much longer. SIWs have growth times less than 1 h and therefore should not remain coherent for a Jovian day. Third, the SIWs require a shear layer at some altitude, whereas the DGWs do not. Finally, the DGWs require forcing in a narrow range of frequencies, whereas the SIWs, since they are self-excited, do not.

Although no Voyager strong methane band imaging exists, the wave packets are visible in multiple filters (violet and orange), as they are in the New Horizons data. Unfortunately, Voyager green and UV filter images were not often acquired; the best images of the region occur at longitudes where waves were not observed in any filter. Using the thermal wind shear at the equator from the Voyager epoch (Figure 2a), there would be very little change in velocity with altitude; from the cloud deck to 90 mbar, the velocity only changes ~5 m/s, so little or no motion would be apparent relative to the background zonal winds in Voyager frames, regardless of the wave altitude. Thus, the Voyager data are not inconsistent with a wave at another altitude. In the Galileo data, the few waves were seen in violet and 756 nm filters, but these regions were not observed in the methane absorption bands at the same time. There are no detailed temperature maps to allow for thermal wind analysis. Lastly, the Voyager and New Horizons images noted in Table S1 imply a wave packet lifetime of more than two Jovian rotations, as features appear at the same latitude and longitude area in images several rotations apart.

The vertical temperature and wind profiles are critical to the formation and propagation of waves with various dispersion relationships (phase velocity, wavelength, wave amplitude, and wavenumber). *Allison* [1990] presented dispersion relationships for various equatorial Rossby, Kelvin, Yanai, and inertia-gravity (I-G) wave modes. I-G waves are the preferred high-frequency mode, with the $j = 1$ harmonic generating eastward waves at the equator (other modes tend to be asymmetric about the equator, see his Figure 6). However, Kelvin modes with $j = -1$ are also possible, and at these high wave numbers (~1473), the I-G mode approaches the Kelvin mode; 90 m/s relative phase velocity for these waves would indicate an equivalent depth of the vertical wave structure of ~350 m (supporting information Figure S1). Another constraint is that each mode has bounding meridional structure or trapping latitudes. Following *Allison* [1990], an I-G wave of this equivalent depth has a trapping latitude ~6.3°, while a Kelvin wave is ~3.7°. The New Horizons waves span ~ ±2° of latitude [*Reuter et al*., 2007], while the Voyager packets are more narrow but appear throughout the equatorial region, as in Figure 3c. Thus, the New Horizons waves are more consistent with a Kelvin wave.

While the QQO drives changes in vertical temperature gradients, and, therefore, stability, I-G and Kelvin waves are also an important component in driving the QQO (and Earth's analog, the QBO), transporting energy vertically [*Li and Read*, 2000; *Baldwin et al*., 2001; *Kawatani et al*., 2010]. Reanalysis of the Galileo probe entry data confirms the presence of vertically propagating waves at all altitudes above 1 bar [*Watkins and Cho*, 2013]. The cloud deck observations of horizontal mesoscale waves may be illustrating key portions of this cycle. In addition, changes in solar insolation, both diurnally and seasonally, may also play a role in wave visibility [*Simon-Miller and Gierasch*, 2010]. Future global circulation and analytical models will need to consider all of these factors to match the observations.

6. Conclusions

This work reanalyzed several spacecraft data sets to better constrain the properties of Jupiter's mesoscale waves: horizontal extent, phase velocity, lifetime, and altitude. In the Voyager and Galileo eras, the mesoscale waves appeared in discrete packets, showing no velocity relative to the cloud-tracked winds.

Voyager data indicate that wave packets may have lifetimes of at least two Jovian rotations, although most wave packets are not visible after a single planet rotation. During the New Horizons encounter, extensive equatorial wave trains having a phase velocity ~90 ± 5 m/s faster than the background tropospheric winds were seen over 20 h at all longitudes. These spanned several degrees of latitude and show indications of shadows at high solar angles.

Existing mesoscale wave models favor longitudinally standing waves, which may be possible if the waves are at an altitude above or below the cloud deck, while dispersion relationships indicate that eastward wave propagation is also possible. Based on the combination of phase velocity, wavelength, and meridional extent, the waves are most consistent with a $j = -1$ K wave with equivalent depth of 350 m. With Juno due to arrive at Jupiter in 2016, observations of the equator with visible and infrared wavelengths will be helpful in further constraining mesoscale wave properties and formation conditions.

Acknowledgments
Work by A.A.S. was funded in part by the NASA Planetary Atmospheres Program. Data are publicly available and were obtained from the Planetary Data System Atmospheres Node (mapped Galileo data) and Rings Node (Voyager 2 and New Horizons LORRI data). We thank R. Morales-Juberias, Andrew Ingersoll, and an anonymous reviewer for providing constructive comments.

The Editor thanks Andrew Ingersoll and an anonymous reviewer for their assistance in evaluating this paper.

References

Allison, M. (1990), Planetary waves in Jupiter's equatorial atmosphere, *Icarus*, *83*, 282–307, doi:10.1016/0019-1035(90)90069-L.

Arregi, J., J. F. Rojas, R. Hueso, and A. Sanchez-Lavega (2009), Gravity waves in Jupiter's equatorial clouds observed by the Galileo orbiter, *Icarus*, *202*, 358–360, doi:10.1016/j.icarus.2009.03.028.

Atkinson, D. H., A. P. Ingersoll, and A. Seiff (1997), Deep winds on Jupiter as measured by the Galileo probe, *Nature*, *388*, 649–650.

Atkinson, D. H., J. B. Pollack, and A. Seiff (1998), The Galileo probe doppler wind experiment: The measurement of the deep zonal winds on Jupiter, *J. Geophys. Res.*, *103*, 22,911–22,928, doi:10.1029/98JE00060.

Baldwin, M. P., et al. (2001), The quasibiennial oscillation, *Rev. Geophys.*, *39*, 179–229, doi:10.1029/1999RG000073.

Bosak, T., and A. P. Ingersoll (2002), Shear instabilities as a probe of Jupiter's atmosphere, *Icarus*, *158*, 401–409, doi:10.1006/icar.2002.6886.

Cheng, A., et al. (2008), Long-range reconnaissance imager on New Horizons, *Space Sci. Rev.*, *140*, 189–215, doi:10.1007/s11214-007-9271-6.

Dyudina, U., et al. (2009), Saturn's south polar vortex compared to other large vortices in the Solar System, *Icarus*, *202*, 240–248, doi:10.1016/j.icarus.2009.02.014.

Flasar, F. M., and P. J. Gierasch (1986), Mesoscale waves as a probe of Jupiter's deep atmosphere, *J. Atmos. Sci.*, *43*, 2683–2707, doi:10.1175/1520-0469(1986)043<2683:MWAAPO>2.0.CO;2.

Kawatani, K. S., T. J. Dunkerton, S. Watanabe, S. Miyahara, and M. Takahashi (2010), The roles of equatorial trapped waves and internal inertia–Gravity waves in driving the quasi-biennial oscillation. Part I: Zonal mean wave forcing, *J. Atmos. Sci.*, *67*, 963–980, doi:10.1175/2009JAS3222.1.

Leovy, C. B., A. J. Friedson, and G. S. Orton (1991), The quasi-quadrennial oscillation of Jupiter's equatorial stratosphere, *Nature*, *354*, 380–382, doi:10.1038/354380a0.

Li, L., A. P. Ingersoll, A. R. Vasavada, A. A. Simon-Miller, A. D. Del Genio, S. P. Ewald, C. C. Porco, and R. A. West (2006), Vertical wind shear on Jupiter from Cassini images, *J. Geophys. Res.*, *111*, E04004, doi:10.1029/2005JE002556.

Li, L., et al. (2013), Strong Temporal Variation Over One Saturnian Year: From Voyager to Cassini, *Sci. Rep.*, *3*, 2410, doi:10.1038/srep02410.

Li, X., and P. L. Read (2000), A mechanistic model of the quasi-quadrennial oscillation in Jupiter's stratosphere, *Planet. Space Sci.*, *48*, 637–669, doi:10.1016/S0032-0633(00)00033-7.

Orton, G., et al. (1991), Thermal maps of Jupiter: Spatial organization and time dependence of stratospheric temperatures, 1980–1991, *Science*, *252*, 537–542, doi:10.1126/science.252.5005.537.

Reuter, D. C., et al. (2007), Jupiter cloud composition, stratification, convection and wave motion: A view from New Horizons, *Science*, *318*, 223–225, doi:10.1126/science.1147618.

Reuter, D. C., et al. (2008), Ralph: A visible/infrared imager for the New Horizons Pluto/Kuiper belt mission, *Space Sci. Rev.*, *140*, 129, doi:10.1007/s11214-008-9375-7.

Salby, M. L. (1996), *Fundamentals of Atmospheric Physics*, Academic Press, New York.

Simon-Miller, A. A., and P. J. Gierasch (2010), On the long-term variability of Jupiter's winds and brightness as observed from Hubble, *Icarus*, *210*, 258–269, doi:10.1016/j.icarus.2010.06.020.

Simon-Miller, A. A., B. J. Conrath, P. J. Gierasch, G. S. Orton, R. K. Achterberg, F. M. Flasar, and B. Fisher (2006), Jupiter's atmospheric temperatures: From voyager IRIS to Cassini CIRS, *Icarus*, *180*, 98–112, doi:10.1006/icar.2002.6886.

Watkins, C., and J. Y.-K. Cho (2013), The vertical structure of Jupiter's equatorial zonal wind above the cloud deck, derived using mesoscale gravity waves, *Geophys. Res. Lett.*, *40*, 472–476, doi:10.1029/2012GL054368.